Strong-Coupling Electrostatics in the Presence of Dielectric Inhomogeneities

Y. S. Jho,[1,2] M. Kanduč,[3] A. Naji,[1,4] R. Podgornik,[3,5] M. W. Kim,[1,2] and P. A. Pincus[1,2]

[1]*Materials Research Laboratory, University of California, Santa Barbara, California 93106, USA*
[2]*Department of Physics, Korea Advanced Institute of Science and Technology, Yuseong-Gu, Daejeon, Korea 305-701*
[3]*Department of Theoretical Physics, J. Stefan Institute, SI-1000 Ljubljana, Slovenia*
[4]*Department of Chemistry and Biochemistry, University of California, Santa Barbara, California 93106, USA*
[5]*Department of Physics, Faculty of Mathematics and Physics, University of Ljubljana, SI-1000 Ljubljana, Slovenia*

(Received 12 May 2008; published 29 October 2008)

We study the strong-coupling (SC) interaction between two like-charged membranes of finite thickness embedded in a medium of higher dielectric constant. A generalized SC theory is applied along with extensive Monte Carlo simulations to study the image charge effects induced by multiple dielectric discontinuities in this system. These effects lead to strong counterion crowding in the central region of the intersurface space upon increasing the solvent-membrane dielectric mismatch and change the membrane interactions from attractive to repulsive at small separations. These features agree quantitatively with the SC theory at elevated couplings or dielectric mismatch where the correlation hole around counterions is larger than the thickness of the central counterion layer.

DOI: 10.1103/PhysRevLett.101.188101 PACS numbers: 87.10.Rt, 82.70.−y

Biological macromolecules such as DNA, lipid membranes and proteins are highly charged in water. Electrostatic interactions play a key role in determining structure, phase behavior and specific functioning of these macroions in aqueous biological media [1]. One particular trait of these systems is that their behavior is dominated, to a large extent, by neutralizing counterions that surround them in a diffuse ionic cloud. When present at higher valencies, these counterions are known to generate strong electrostatic attractions between like-charged macroions as observed in numerous experiments and simulations [2]. These observations stand in stark contrast with the traditional mean-field or Poisson-Boltzmann (PB) theories, which predict purely repulsive forces [1].

Consequently, there have been a number of attempts to assess corrections to the PB theory using, e.g., correlated density fluctuations around the mean-field ionic distribution or additional nonelectrostatic interactions [3,4]. An alternative approach has been developed recently [2,5–9], which leads to the so-called strong-coupling (SC) theory; it is known to become exact in the limit of high macroion charge, large counterion valency, low medium dielectric constant or low temperature, where the PB theory breaks down.

While the strong-coupling phenomena are well understood in the framework of the SC theory, it still remains a challenge to predict the behavior of realistic biophysical systems, which, among other things, exhibit highly inhomogeneous dielectric structure. The large difference in static dielectric constants of water ($\varepsilon \simeq 80$), being the most common solvent, and the nonpolar moieties ($\varepsilon \simeq 2$–5), comprising the molecular interiors of proteins, lipid membranes and DNA, leads to substantial differences in interactions between charges in most common biological environments. Moreover, the presence of a combination of both aqueous and hydrocarbon regions in the immediate surrounding (as, e.g., in the case of two or more interacting lipid membranes) leads to a more complex pattern of *image charges* that are induced by multiple dielectric discontinuities in the system.

In this Letter, we consider a system of two like-charged membranes of finite thickness in a medium of higher dielectric constant and determine the counterion distribution and the interaction between the membranes by means of both Monte Carlo simulations and a generalized SC theory. Recent studies show that image interactions in highly charged systems could result in remarkable effects such as in the surface adsorption of flexible polyelectrolytes [10] and the charge inversion of macroions [11]. In the slab geometry, the dielectric discontinuity effects have been studied in both weak-coupling [9,12–16] and strong-coupling regimes [9,14,16,17]. These works, however, deal with one or two semi-infinite slabs and do not consider the finite thickness of the membranes or the multitude of images produced in the two-slab system. While accounting only for the first-order images serves as an accurate approximation at low couplings [9,12,14], the same approximation as we show breaks down on a qualitative level at elevated couplings, where the higher-order induced images play an essential role. For vanishing membrane thickness (no dielectric discontinuity), the long-range SC attraction mediated by counterions is dominant and leads to a tightly bound state between two like-charged membranes [8,9]. This well-known picture changes as the membrane thickness and the solvent-membrane dielectric mismatch increase, leading to enhanced repulsive (and even change from attractive to repulsive) interaction between membranes at small separations. This SC repulsion depends strongly on the dielectric mismatch contrary

 © 2008 The American Physical Society

to the (repulsive) PB interaction which is not affected by the image charges.

Let us consider two charged parallel membranes of thickness b and dielectric constant ε_1 with their inner surfaces being located at $z = \pm a$ and bearing uniform charge density $-\sigma e$ (Fig. 1). The system is immersed in a solution of dielectric constant ε_2 containing $+q$-valent counterions. Apart from the direct contribution from the charged surfaces, the electrostatic potential experienced by each counterion also involves contributions from image charges induced at each solvent-membrane interface. We shall consider the contribution from all image charges in the present geometry. To this end, we have developed a new numerical algorithm that enables one to compute efficiently the electrostatic interactions in the presence of multiple dielectric discontinuities [18]. Assuming two-dimensional lateral periodicity (in the plane of the membranes), we combine the image charge method with the MMM2D summation technique to obtain fast-converging series for evaluating Coulombic interactions [17,19].

The state of the system may be described in terms of the following dimensionless parameters: the *dielectric jump parameter* $\Delta = (\varepsilon_2 - \varepsilon_1)/(\varepsilon_2 + \varepsilon_1)$, the rescaled half-distance $\tilde{a} = a/\mu$, the rescaled thickness $\tilde{b} = b/\mu$, and the *electrostatic coupling parameter* $\Xi = q^2\ell_B/\mu$, where $\mu = 1/(2\pi q\ell_B\sigma)$ is the so-called Gouy-Chapman length and $\ell_B = e^2/(4\pi\varepsilon_2\varepsilon_0 k_B T)$ is the Bjerrum length [1,2]. The coupling parameter Ξ determines the strength of electrostatic correlations: for dielectrically homogeneous systems, the SC behavior dominates typically for $\Xi > 10$, while the PB description is found to be valid at small couplings $\Xi < 1$ [2,8,9].

For a typical membrane with $\sigma e \simeq 1\,\frac{e}{\mathrm{nm}^2}$ in water ($\varepsilon_2 \simeq 80$ at room temperature), we have $\Xi \simeq 3, 25, 85$ and 200 by choosing counterion valency as $q = 1, \ldots, 4$, respectively. Higher couplings may be obtained by using less dielectric solvents (e.g., mixtures containing methanol, $\varepsilon_2 \simeq 33$) since $\Xi \sim 1/\varepsilon_2^2$. Here we shall focus mainly on the SC regime with large Ξ and vary Δ (at fixed $\varepsilon_2 = 80$) in the range $\Delta = 0$ (no discontinuity, $\varepsilon_1 = 80$) to $\Delta = 0.95$ (water/hydrocarbon interface, $\varepsilon_1 = 2$).

In Fig. 2(a), we show simulated counterion density profiles between two membranes of thickness $b/\mu = 100$ and coupling parameter $\Xi = 100$ as Δ varies (symbols). As seen, counterions are strongly depleted from the vicinity of the charged surfaces and accumulate around the midplane as the dielectric mismatch is increased—a trend observed also in studies that include only the first induced images [9,12]. This behavior is intimately connected with the electrostatic correlations, i.e., it will be absent in the PB limit $\Xi \to 0$ [see Fig. 2(c)]. Intuitively, for $\varepsilon_2 > \varepsilon_1$ counterions have the same sign as their images and the counterion-image repulsion provides the mechanism for the foregoing observation in the SC regime.

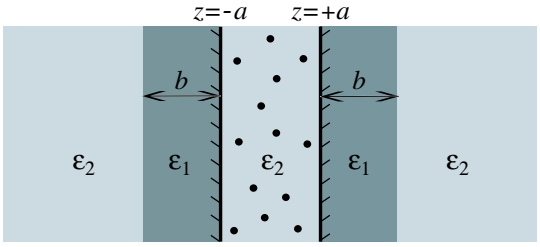

FIG. 1 (color online). Schematic view of two charged membranes and counterions in between. Here $2a$ is the closest-approach distance (leaving out the counterion diameter from the actual distance) and counterion excluded-volume repulsions are neglected.

In general, the origin of SC phenomena goes back to the fact that at large couplings, $\Xi \gg 1$, counterions strongly repel each other and tend to form a highly correlated quasi-2D layer close to a charged surface. Thus, individual ions become increasingly "isolated" as they are surrounded by a large correlation hole of size $a_\perp^2 \sim q/\sigma$ (or $a_\perp/\mu \sim \sqrt{\Xi}$) as follows from the local electroneutrality condition [9]. As a result, the single-particle interaction between individual counterions (including their own images) and the charged membranes, $u(\tilde{z})$, is expected to dominate and lead to a barometric number density profile, $\rho_{SC}(z)$, for counterions; in rescaled units $\tilde{\rho}_{SC}(\tilde{z}) \equiv \frac{\rho_{SC}(z)}{4\pi\ell_B\sigma^2} = A(\tilde{a})e^{-u(\tilde{z})}$, where $\tilde{z} = z/\mu$ and $1/A(\tilde{a}) = \int_{-\tilde{a}}^{\tilde{a}} d\tilde{z}\tilde{\rho}_{SC}(\tilde{z})$. For $\Delta = 0$, this result indeed follows as an exact limiting ($\Xi \to \infty$) result from a systematic $1/\Xi$-expansion [2,8], giving a *uniform* profile $\tilde{\rho}_{SC}(\tilde{z}) = \frac{1}{2\tilde{a}}$ (with $u(\tilde{z}) = 0$ and $A(\tilde{a}) = \frac{1}{2\tilde{a}}$) in agreement with our simulations [horizontal line in Fig. 2(a)]. Higher-order terms in general involve corrections due to counterion-counterion interactions at finite Ξ [8].

For an inhomogeneous system with $\Delta > 0$, we generalize the $1/\Xi$-expansion method by taking into account the presence of all four dielectric boundaries (Fig. 1) and obtain the leading-order ($\Xi \to \infty$) SC density profile as

$$\tilde{\rho}_{SC}(\tilde{z}) = A(\tilde{a})\exp\left(-\Xi\int_0^\infty dQ\,\frac{\cosh 2Q\tilde{z}}{\Delta_Q^{-1}e^{2Q\tilde{a}} - \Delta_Q e^{-2Q\tilde{a}}}\right), \tag{1}$$

where $\Delta_Q = \Delta\frac{1-\exp(-2Q\tilde{b})}{1-\Delta^2\exp(-2Q\tilde{b})}$. This result is plotted in Fig. 2(a) (solid lines) and is in excellent agreement with our data (symbols) for all dielectric jump parameters at $\Xi = 100$. Qualitatively, the bellshaped profiles may be approximated for large b by the first-image expression

$$\tilde{\rho}_{SC}(\tilde{z}) \simeq A(\tilde{a})\exp\left(-\frac{\Delta\Xi\tilde{a}/2}{\tilde{a}^2 - \tilde{z}^2}\right). \tag{2}$$

The SC pressure acting on each membrane may be calculated from $\tilde{P}_{SC} \equiv P_{SC}/(2\pi\ell_B\sigma^2 k_B T) = -\partial\tilde{\mathcal{F}}_{SC}/\partial\tilde{a}$ by evaluating the SC free energy $\tilde{\mathcal{F}}_{SC}$ (per $k_B T$ and number of counterions) using standard SC methods [9,16]; hence

$$\tilde{\mathcal{F}}_{SC} = \tilde{a} - \ln\int_0^{\tilde{a}} d\tilde{z}\exp\left(-\Xi\int_0^\infty dQ\,\frac{\cosh 2Q\tilde{z} + \Delta_Q e^{-2Q\tilde{a}}}{\Delta_Q^{-1}e^{2Q\tilde{a}} - \Delta_Q e^{-2Q\tilde{a}}}\right). \tag{3}$$

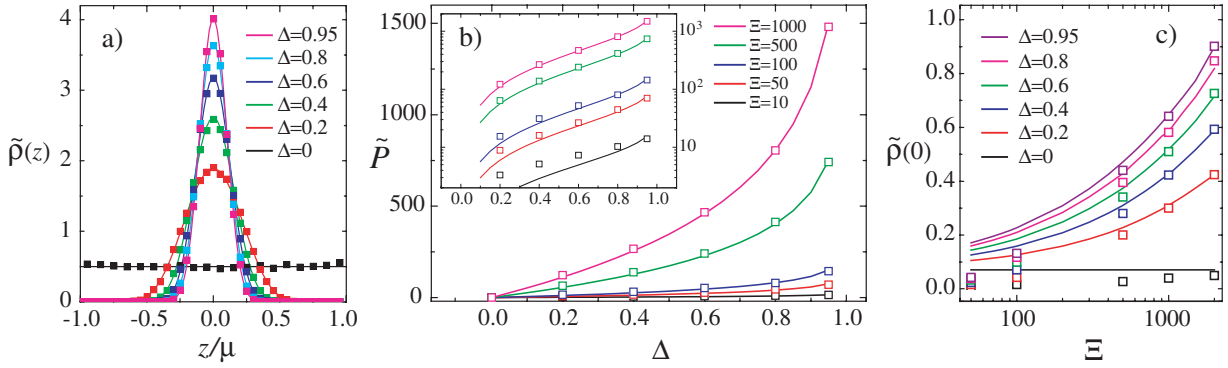

FIG. 2 (color online). (a) Rescaled counterion density profile between two like-charged dielectric membranes for $\Xi = 100$, $b/\mu = 100$, $a/\mu = 1$ and as the dielectric mismatch Δ is increased (from bottom to top at $z = 0$). (b) Rescaled intermembrane pressure as a function of Δ for $b/\mu = 100$, $a/\mu = 1$ and as Ξ is increased (bottom to top); inset shows the details in the logarithmic scale. (c) The midplane ($z = 0$) counterion density, $\tilde{\rho}(0)$, as a function of the coupling parameter Ξ for $a/\mu = 7$, $b/\mu = 100$ and as Δ is increased (bottom to top). In (a)–(c) lines are the SC predictions (see the text) and symbols are simulation data.

The first term is the SC energetic attraction induced by single counterions between the two surfaces when there are no images ($\Delta = 0$) [8,9]. The second term includes the counterion confinement entropy as well as the image charge contributions. For $\Delta = 0$, this second term reduces to the entropic $\ln \tilde{a}$ term as expected and the SC pressure follows as $\tilde{P}_{\rm SC} = -1 + 1/\tilde{a}$, featuring repulsion at small separation, $a < a_*$, and attraction at large separation, $a > a_*$, with $a_*/\mu = 1$ being the stable equilibrium (zero-pressure) half-distance. Upon increasing Δ, the intermembrane pressure becomes increasingly more repulsive at small separations due to the counterion-image repulsions; it may be increased by up to an order of magnitude as shown by the data in Fig. 2(b) (symbols). This behavior is captured quantitatively by the SC pressure, $\tilde{P}_{\rm SC}$ [solid lines, obtained from Eq. (3)] for high enough couplings at all values of the dielectric jump.

So far, we have considered only small membrane separations $a \sim \mu$, where good agreement with the SC predictions is achieved for $\Xi \sim 100$ and larger couplings. Formally, the SC theory is exact for all separations when $\Xi \to \infty$. But for finite Ξ as is the case in simulations, this limiting single-particle description is expected to perform poorly at large separations, where the subleading counterion-counterion interactions play a more significant role [8]. For $\Delta = 0$, the SC validity regime is identified as $a \ll a_\perp$ or $\tilde{a} \ll \sqrt{\Xi}$ [2,9], i.e., when the surface separation is smaller than the counterion spacing, $a_\perp$, defined above. In the presence of images, counterions are crowded in a thin layer of thickness (or the full width at half maximum) $\delta_z < a$ around the midplane [Fig. 2(a)]. From Eq. (2) the thickness δ_z may be estimated as $\delta_z = a[1 - (1 + 2a \ln 2/\Xi\Delta)^{-1}]^{1/2}$. The SC theory is expected to hold when $a_\perp$ is larger than δ_z, i.e., when counterions form a quasi-2D layer. Hence, we find the generalized criterion $\delta_z \ll a_\perp$ or (in rescaled units)

$$\tilde{a}^3 \ll \tilde{a}\Xi + \Delta\Xi^2. \tag{4}$$

Thus, for the SC theory to be valid at larger a, a larger coupling parameter or dielectric mismatch is needed. Moreover, this predicts that the SC theory remains valid for a *larger* range of separations when Δ is nonzero.

In Fig. 2(c) we show the midplane density $\tilde{\rho}(0)$ as a function of Ξ for a larger half-distance $a/\mu = 7$. The SC theory (solid lines) is no more valid for $\Xi \lesssim 100$, largely overestimating the simulated density (symbols). This reflects the fact that counterion-counterion repulsions absent in the leading-order theory are not negligible and tend to drive the counterions away from the crowded midplane toward the surfaces. The same trend also transpires in the pressure data for $a/\mu = 7$ [Fig. 3(a)], where good agreement is obtained only for $\Xi \gtrsim 500$.

The theoretical and numerical results are generally found to be in better agreement for larger Δ as expected from Eq. (4); see Figs. 2(b) (inset), 2(c) and 3(a) (inset). The change from attractive to repulsive interaction upon increasing Δ is more clearly seen in Fig. 3(a).

In the presence of dielectric inhomogeneities not only the strength of the intermembrane repulsion becomes larger but also its range increases, pushing the attraction regime and the equilibrium separation, a_*, to larger distances. When $\Delta = 0$, as noted above, $\tilde{a}_* = a_*/\mu = 1$ in agreement with our simulations in Fig. 3(b). For $\Delta > 0$, $\tilde{a}_*$ shows a monotonic increase with the coupling parameter. While the qualitative trend is reproduced by the SC theory, the quantitative agreement between simulated $\tilde{a}_*$ (symbols) and the theoretical predictions (solid lines) is obtained only for small to intermediate Δ. In general, the SC theory underestimates the $\tilde{a}_*$ values [by $\lesssim 20\%$ in Fig. 3(b)]. This discrepancy reflects the interplay between counterion-image repulsions (included in both theory and simulations) and counterion-counterion repulsions (included only in the simulations): as Δ increases, the former grows pushing a_* to larger values beyond the regime of validity of the SC theory [Eq. (4)], where the latter effects need to be accounted for as well. A similar trend is found when membrane thickness is increased.

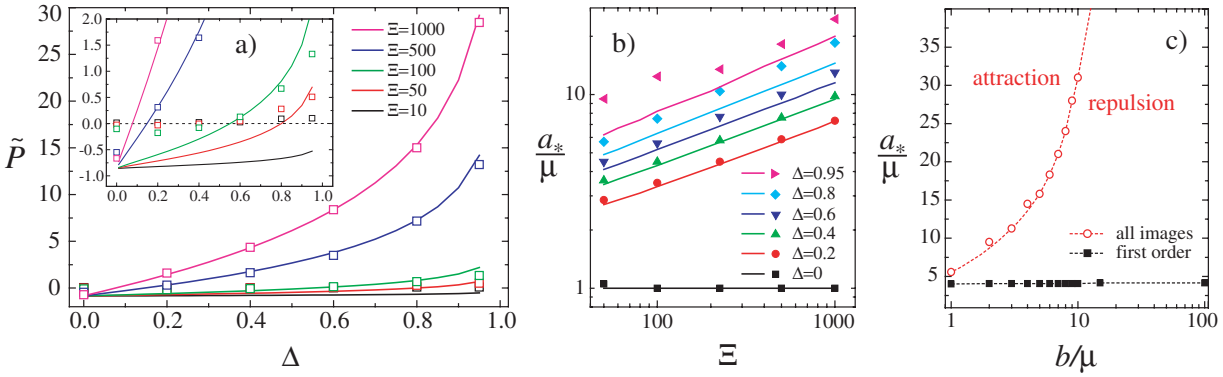

FIG. 3 (color online). (a) Same as Fig. 2(b) but for $a/\mu = 7$. Inset shows the details for small pressures. (b) Simulated equilibrium half-distance, a_*, as a function of Ξ for $b/\mu = 2$ and as Δ is increased. Lines are SC predictions [from minimization of Eq. (3)]. (c) Simulation results for a_* as a function of b with all images (circles) and the first-order images only (squares) for $\Xi = 50$ and $\Delta = 0.95$ (the latter shows a very weak increase with b); here lines are guides to the eye. The surfaces attract for $a > a_*$ and repel for $a < a_*$.

Note that while the weak-coupling results are less sensitive to the dielectric jump effects, a remarkable dependence on Δ is found in the SC regime [Figs. 2(b), 2(c), and 3(a)]. Since the SC interactions are long-ranged [within the regime defined by Eq. (4)], a larger number of induced images are needed to be taken into account in the SC regime. The first-order-image approximation [9,12] fails qualitatively at high couplings and particularly for thick membranes as it always predicts a strong attraction and a remarkably different (smaller) a_* as shown in Fig. 3(c).

In conclusion, we have shown that the generalized SC theory can explain the effects of dielectric inhomogeneity in the two-slab system at elevated couplings (specified by an extended SC criterion), where counterions are strongly depleted from the interfacial regions leading to enhanced repulsive intermembrane interactions. Thus in contrast to weakly coupled systems, the electrostatics of highly coupled systems can be affected significantly by the image charges. As an experimentally measurable effect, the SC images may lead to swelling of the multilamellar lipid arrays upon changing the solvent dielectric constant. In reality, however, one deals with additional factors such as smooth dielectric profiles and discrete surface charges [14,15,17], which offer interesting problems for a more detailed study in the future.

Y. S. J., P. A. P. and M. W. K. acknowledge funds from the National Science Foundation (Grants DMR-0503347, DMR-0710521) and MRSEC NSF DMR-0520415. Y. S. J. and M. W. K. have been supported by the KISTEP (Grant I-03-064) and the Korea Health 21 R&D Project, and M. K. and R. P. by the Agency for Research and Development of Slovenia (Grants P1-0055(C), Z1-7171, L2-7080).

[1] W. C. K. Poon and D. Andelman, *Soft Condensed Matter Physics in Molecular and Cell Biology* (Taylor & Francis, London, 2006).

[2] H. Boroudjerdi, Y.-W. Kim, A. Naji, R. R. Netz, X. Schlagberger, and A. Serr, Phys. Rep. **416**, 129 (2005).

[3] R. Podgornik and B. Žekš, J. Chem. Soc., Faraday Trans. 2 **84**, 611 (1988); P. A. Pincus and S. A. Safran, Europhys. Lett. **42**, 103 (1998); see also [2,8] and references therein.

[4] Y. Burak and D. Andelman, J. Chem. Phys. **114**, 3271 (2001).

[5] I. Rouzina and V. A. Bloomfield, J. Phys. Chem. **100**, 9977 (1996).

[6] A. Y. Grosberg, T. T. Nguyen, and B. I. Shklovskii, Rev. Mod. Phys. **74**, 329 (2002).

[7] Y. Levin, Rep. Prog. Phys. **65**, 1577 (2002).

[8] R. R. Netz, Eur. Phys. J. E **5**, 557 (2001); A. G. Moreira and R. R. Netz, *ibid.* **8**, 33 (2002).

[9] A. Naji, S. Jungblut, A. G. Moreira, and R. R. Netz, Physica A (Amsterdam) **352**, 131 (2005).

[10] R. R. Netz and J.-F. Joanny, Macromolecules **32**, 9013 (1999); **32**, 9026 (1999).

[11] T. T. Nguyen, A. Yu. Grosberg, and B. I. Shklovskii, J. Chem. Phys. **113**, 1110 (2000); T. T. Nguyen and B. I. Shklovskii, Phys. Rev. E **64**, 041407 (2001).

[12] D. Bratko, B. Jönsson, and H. Wennerström, Chem. Phys. Lett. **128**, 449 (1986); R. Kjellander and S. Marčelja, *ibid.* **112**, 49 (1984).

[13] R. Menes, P. A. Pincus, and B. Stein, Phys. Rev. E **62**, 2981 (2000); J. Schmit, R. Menes, and P. A. Pincus, *ibid.* **66**, 061502 (2002).

[14] A. G. Moreira and R. R. Netz, Europhys. Lett. **57**, 911 (2002).

[15] S. Taheri-Araghi and B.-Y. Ha, Phys. Rev. E **72**, 021508 (2005).

[16] M. Kanduč and R. Podgornik, Eur. Phys. J. E **23**, 265 (2007).

[17] Y. S. Jho, G. Park, C. S. Chang, P. A. Pincus, and M. W. Kim, Phys. Rev. E **76**, 011920 (2007).

[18] Y. S. Jho, F. L. H. Brown, M. W. Kim, and P. Pincus, J. Chem. Phys. **129**, 134511 (2008).

[19] A. Arnold and C. Holm, Comput. Phys. Commun. **148**, 327 (2002).